AN ASSESSMENT ON THE STABILITY PERFORMANCE OF A PWR WITH ATF

JAVIER RIVEROLA GURRUCHAGA, SANTIAGO ALVAREZ MANZANEDO

Department of Fuel Operations Engineering, ENUSA Industrias Avanzadas, S.A.
C/ Santiago Rusiñol 12, 28040 Madrid, Spain

ABSTRACT

This paper evaluates the dynamic performance of different accident tolerant fuel (ATF) designs against reactivity steps and other time varying inputs. Stability of the nuclear system is assessed both in the time dominion and frequency dominion with classic methods of linear stability analysis. The point kinetics open loop and closed loop transfer functions with feedbacks are examined to obtain the pole/zero configuration of the characteristic equation of the dynamic system, phase and gain margins, and peak and resonance frequency on a Bode and Nichols representations.
In this work, a typical 17x17 12 feet / three loop PWR with standard cell and core geometry is taken as reference. Results of the dynamic analysis show that inherent stability in a wide range of operating range is guaranteed. This work confirms again the self-regulating capability of PWR due to the dynamic combination of fuel and moderator reactivity effects also with nonstandard fuel lattices.

1. Introduction

Today, the nuclear industry is making great R+D efforts to attain an alternative fuel-cladding that combines enhanced performance during a heat transfer accident with acceptable manufacturability. This new fuel is intended to replace the current the UO2 ceramic pellet inside a zirconium alloy.
Among the many different options investigated, a few of them are already being placed for manufacturing, testing, licensing and LTA irradiation roadmaps. In the pellet side, alternatives with elevated thermal conductivity and diffusivity as well as higher loading of uranium are chosen. As for the cladding, several materials that exhibit enhanced mechanical and chemical resistance have been proposed. In this paper, we have investigated twelve combinations corresponding to three fuel materials and four cladding materials.
If the reactivity perturbation is moderated (less than prompt critical), PWR are inherently stable in a wide range of operating conditions. Feedbacks due to fuel and moderator temperature change are dynamically negative, which is a guarantee of asymptotic stability. Current evaluations are usually based in exhaustive use of computer simulation by solving the space-time thermal and kinetics equations in the time domain and in the neighbourhood of the equilibrium point. Instead, this paper goes back to fundamentals and relies on classic methods of linear stability and dynamics analysis in the time and frequency domains for the twelve fuel-cladding combinations discussed below, see Table 1.

2. Accident tolerant fuel options

2.1 Cladding Materials

Zirconium alloys. current 2nd generation LWR fuel cladding is made of zirconium with some alloying elements as Sn or Nb. The main advantage of this material is the very low neutron absorption cross section, but it quickly reacts with steam at high temperature as in the case of a LOCA. This oxidation behaviour can be improved with a sort of coating layer (Cr or Ti2Al).

Silicon carbide composite SiC CMC. Because of its feasibility as LWR cladding, this is one of the cladding options currently tested in the industry. SiC nice properties are very low neutron absorption, no steam oxidation up to high temperature, very low oxidation rate during steady state operation and stable geometry. However, it exhibits low heat conductivity, poor tightness,

and properties dependence on irradiation. Besides, SiC exhibits a marked increase in the oxidation rate in water steam environments at circa 1400 ºC resulting in carbon oxide and a protective layer of silica. In practice, SiC designs include an inner monobloc layer and an external fibre layer to provide both tightness and ductility respectively. Typically, SiC CMC cladding is thicker than standard Zr or SS cladding. In this work, we assume a thickness of 0.74 mm (30% increase over Zr).

Austenitic Steel. Cr - Ni alloy is also a good option for nuclear fuel cladding because of its manufacturability and great industrial experience, but it requires thinner cladding to compensate the relatively large neutron absorption cross section. Besides, it melts at a somewhat low temperature and it is susceptible to stress corrosion cracking. Considerable research is done to improve these disadvantages. Other steel options like Ferritic-martensic alloys or other, not susceptible to stress corrosion cracking, may play an important role.

2.2 Ceramic Fuel Materials

Uranium dioxide UO2. There is plenty of experience in UO2 utilization in all nuclear fuel cycle stages from manufacturing, exposure and disposal. It is today´s reference in most of nuclear reactors worldwide. However, it exhibits a poor heat transmission, which becomes even worse as burnup increases.

Uranium silicide U3Si2. With superior heat transmission and greater fissile content than UO2, this material is a potential replacement for UO2. However, the melting temperature is comparatively low and it shows a trend to swell. Since no oxygen exists in the fuel as component, oxidation does not develop in the inner side of the cladding. There are research testing programs in place in order to evaluate the benefits and drawbacks of this material.

Uranium nitride UN. This ceramic material has a rather high thermal conductivity and melting point, no constituent oxygen, and good retention of fission products. Drawbacks are the need of water proofing to avoid an eventual reaction with cooling water. Besides, in order to prevent N14 (n,p) C14 reactions, there is a need of enriching in favour of N15, which is an expensive process. It is currently used in LWR in TRISO form.

Uranium carbide UC. Another interesting refractory ceramic material with very high thermal conductivity and melting point, great use experience in reactors and lack of constituent oxygen. Nevertheless, UC has a vigorous reaction with water and steam at high temperature, so its applicability is restricted to specific environments. It is commonly used in pebble bed reactors and particle accelerators.

Table 1 and Figure 1 list the relevant thermo physical properties of these materials as reported in available references [1] to [6].

Material	Density (Kg/m3)	Specific heat (J/Kg K)	Conductivity (W/m K)
Cladding			
Zirconium alloy	6560	293	17.4
SiC	3000	1000	20.0
Austenitic Steel	7755	548	19.0
Fuel (95% TD)			
UO2	10230	307	See Fig. 1
U3Si2	12200	290	15.0
UN	13433	233	See Fig. 1
UC	12559	244	See Fig. 1

Tab 1: Material properties for cladding and fuel in the temperature range of interest.

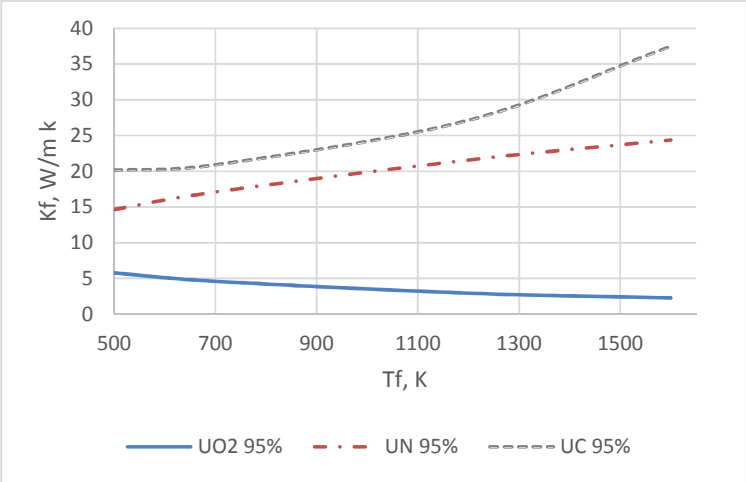

Fig 1. Thermal conductivity versus fuel temperature for various fuel materials.

3. The model

Public literature gathers a number of different models suitable for stability analysis with a variety in the degree of complexity [7, 8]. In this paper, the point kinetics equations with six delayed groups along with lumped parameter thermal models for the fuel, moderator, and a closure relation for the reactivity provide a simple model as follows:

$$\frac{dP}{dt} = \frac{\rho-\beta}{\Lambda} P + \sum \lambda_i C_i \tag{1}$$

$$\frac{dC_i}{dt} = \frac{\beta_i}{\Lambda} P - \sum \lambda_i C_i \qquad \text{i=1,…,6} \tag{2}$$

$$m_f cp_f \frac{dT_f}{dt} = P - UA\left(T_f - T_c\right) \tag{3}$$

$$m_c cp_c \frac{dT_c}{dt} = UA\left(T_f - T_c\right) - 2W_c cp_c (T_c - T_i) \tag{4}$$

$$\rho \cong \alpha_f \left(T_f - T_{f0}\right) + \alpha_c (T_C - T_{C0}) + \rho_{ext} \tag{5}$$

where P is the reactor power, ρ is the reactivity, β is the delayed neutron fraction, Λ is the mean generation lifetime, λ is the delayed neutron decay constant, and C is the precursor density. Besides, mf is the total mass of fuel, cpf is the specific heat of fuel, Tf is the fuel temperature, mc is the coolant mass inside the core, cpc the water specific heat, Tc is the coolant (water) temperature, Ti the core inlet temperature, Wc is the core mass flow rate, and αf and αc, are the fuel and coolant coefficients of reactivity.

In order to obtain a manageable system of equations, the nine ordinary differential equations are linearized around the equilibrium point [p0, c0, Tf0, Tc0] so that the Laplace transform can be applied. After isolating variables and some algebraic handling, the following expressions for the reactivity-to-power G(s), and the power-to-feedback reactivity H(s) are obtained:

$$\boldsymbol{G(s)} = \frac{\delta P}{\delta \rho} = \frac{\frac{1}{s} P_0}{\Lambda + \sum \frac{\beta_i}{s+\lambda_i}} \tag{6}$$

$$\delta T_f = \frac{m_c cp_c s + 2W_c cp_c + UA}{m_f cp_c s(m_c cp_c s + 2W_c cp_c + UA) + UA(m_c cp_c s + 2W_c cp_c)} \delta P \tag{7}$$

$$\delta T_c = \frac{UA}{m_f cp_c s(m_c cp_c s + 2W_c cp_c + UA) + UA(m_c cp_c s + 2W_c cp_c)} \delta P \tag{8}$$

$$\boldsymbol{H(s)} = \alpha_f \delta T_f + \alpha_w \delta T_w \quad (9)$$

$$\boldsymbol{T(s)} = \frac{G(s)}{1 - G(s) \cdot H(s)} \quad (10)$$

The final model is set by equations (6) to (10). Further, expressions (7) and (8) can be simplified in terms of time delays for suitable handling in a dynamics system analysis code,

$$\boldsymbol{\delta T_f} \cong \frac{\boldsymbol{K_{PTf}}}{(\boldsymbol{\tau_f s + 1})} \cdot \delta P, \text{ and} \quad (11)$$

$$\boldsymbol{\delta T_c} \cong \frac{\boldsymbol{K_{PTc}}}{(\boldsymbol{\tau_c s + 1}) \cdot (\boldsymbol{\tau_m s + 1})} \cdot \delta P \quad (12)$$

where, KPTF, KPTC, are the steady state gains for fuel temperature, moderator temperature, and τf, τc, and τm, are the fuel, coolant, and moderator flow time delays.

In this work, a typical 17x17 12 feet / three loop PWR with standard cell and core geometry is taken as reference with parameters in Table 2. These values were calculated in ENUSA with licensed nuclear design and fuel rod codes that consider the relevant input data for geometry and properties. The coefficients of reactivity deserve special mention.

The fuel temperature coefficient, or Doppler coefficient is due to the broadening of U-238 resonances in the absorption cross section as the temperature increases and it follows a Tf^{-2} law. All combinations studied in this paper considers the same U-238/U-235 relative amounts, and the most extreme temperature difference, that is between UO2 and U3Si2, leads to a maximum increase of just +12% over the case of UO2. Therefore, as a fair approximation, one can use the same Doppler coefficient for all cases.

The moderator temperature coefficient MTC, depends mainly on the number density of hydrogen in the coolant, which in turn depends on the water temperature and boron concentration. It is quite valid to assume the same MTC for all cases.

Parameter	**Value**
Reactor power	2940 MW
Delayed neutron fraction, *β*	0.00543
Mean generation lifetime, *Λ*	15 E-6 s
Delayed neutron decay time, *λ*	0.087 s
Core mass flow rate, *Wc*	12 761 kg/s
Doppler coefficient, *αf*	-2.5 pcm/ºC
Moderator temperature coefficient MTC, *αc*	0 to -72 pcm/ºC

Tab 2: Reference reactor parameters and reactivity coefficients

Figure 2 shows a block diagram about the model operating, which includes the nuclear model (yellow blocks), the mechanic model (green block) and the coupled N-thermo hydraulic model (red blocks).

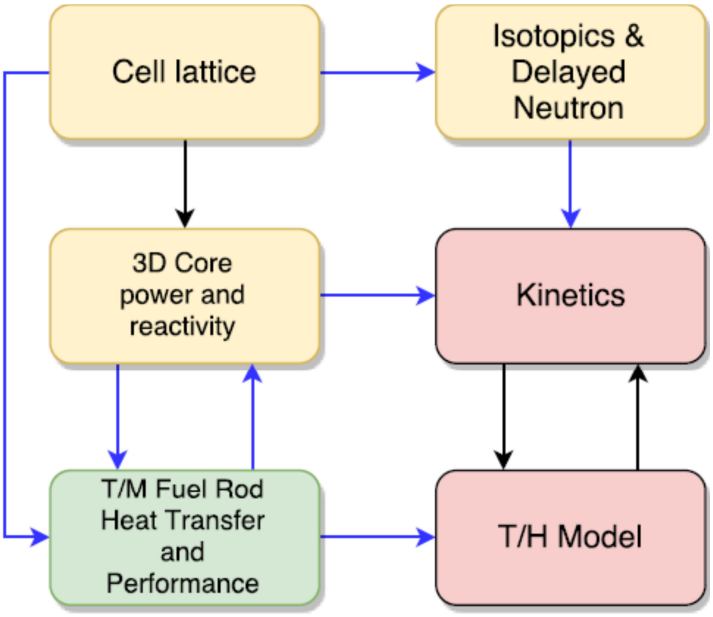

Fig 2: Operating model.

4. Stability analysis of ATF

4.1 Time domain analysis

4.1.1 Poles of the total transfer function T(s)

In order to study the stability of the system, we can check for the roots of the denominator of the transfer function T(s), or poles. The denominator is known as the characteristic equation of the dynamic system,

$$1 - G(s)\cdot H(s) = 0. \qquad (13)$$

The nine degree of freedom model above results in nine poles for each reactor state and fuel. We studied the different combinations of fuel-cladding both at BOC and EOC, and we found that the real part of each pole is negative in all twelve cases, which indicates that the reactor system is asymptotically stable, so the dynamic response to a reactivity perturbation is always bounded. Besides, we observe that these configurations exhibit paired-conjugated poles, especially at EOC, see Table 3. However, the argument is always far greater than +- 90º so any oscillation will be small or even unnoticeable. This outcome can be easily verified in the next section.

The method of poles is equivalent to the method of finding the eigenvalues of the Jacobian matrix of equations (1) to (4).

4.1.2 Response to a reactivity step

We perturbed the dynamic model by a reactivity step input, with an arbitrary +100 pcm height. In all twelve fuel-cladding pairs, the time response to the step followed a similar performance: after a prompt jump proportional to 1/β, negative feedback effects take place and the power becomes stabilized after a few second delay, with no great differences between the smoothest and peaked responses. No sustained oscillation was observable at all.

Figure 3 displays the response for the simulated cases.

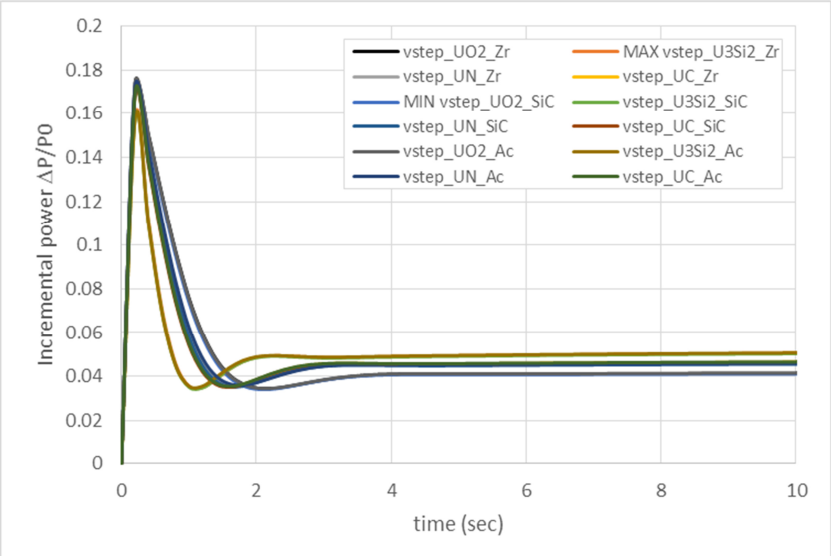

Fig 3. Response to a +100 pcm step.

4.2 Frequency domain analysis

4.2.1 Bode´s diagram

Let´s recall the closed loop transfer function T(s). It is useful to substitute the s variable of the T by jω to obtain the complex response in the frequency domain. Figures 4 and 5 display the magnitude and phase of the closed loop transfer function T(jω) in terms of the frequency of the input signal for two cases (U3Si2+Zr and UO2+SiC) that bound all the other ones.

The magnitude peak in all twelve fuel-cladding combinations is rather low compared to typical peaks for other reactor designs like BWR, see Table 3. Besides, the phase plot does not exhibit a sudden sign change at that frequency which would be the case of a marked resonance. Thus, these dynamic systems do not differ greatly from the corresponding to standard UO2 + Zr fuel. The magnitude plot exhibits a peak around 0.5 Hz, which is the typical natural N-TH frequency of a reactor. This frequency is well below the noise with external and internal origin, from 2 Hz to nearly 100 Hz (control rods, fuel assemblies, core barrel, steam generators, pumps, flow …).

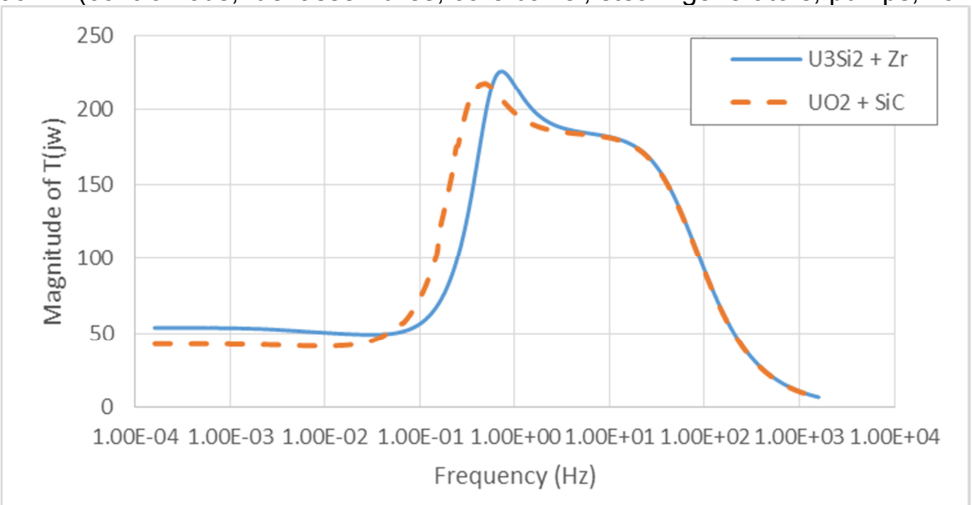

Fig 4. Bode - Magnitude plot of T(jw) of the two bounding cases

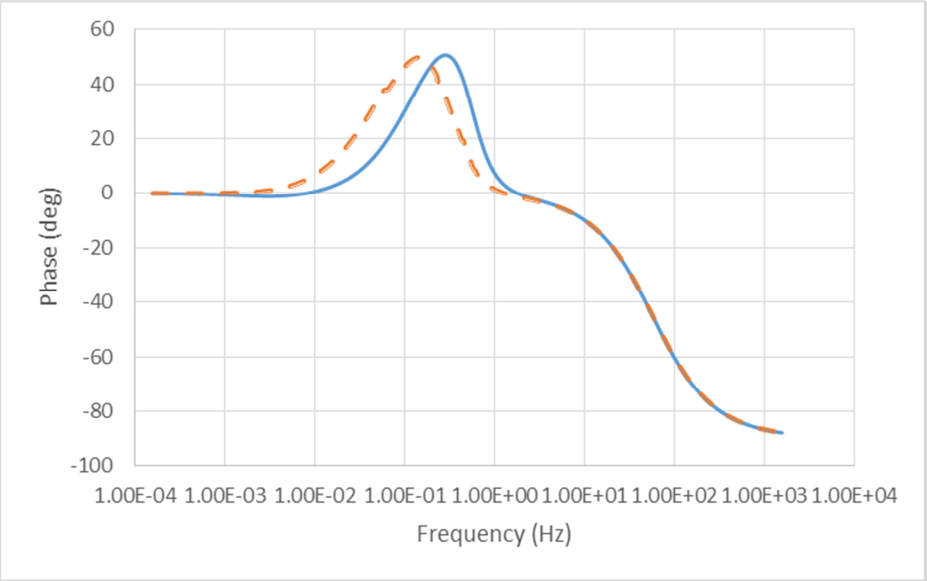

Fig 5. Bode - Phase plot of T(jw) of the two bounding cases

4.2.2 Phase and Gain Margins

Just looking at the total transfer function T(jw) in equation (10), we can see that instability occurs when the modulus of the open loop transfer function G·H is 1 and the phase is 180º simultaneously. It is practical to represent both parameters [Magnitude, Phase] in a Nichols diagram, as the frequency sweeps from zero to infinite. Figure 6 shows the case of U3Si2 + SiC, which reveals the lowest margins for all twelve cases. We can see that in this case and all the other cases, the margin of the locus to the critical point [1,-180º] is very large, as expected in PWR type fuel. Table 3 compiles again the gain and phase margin.

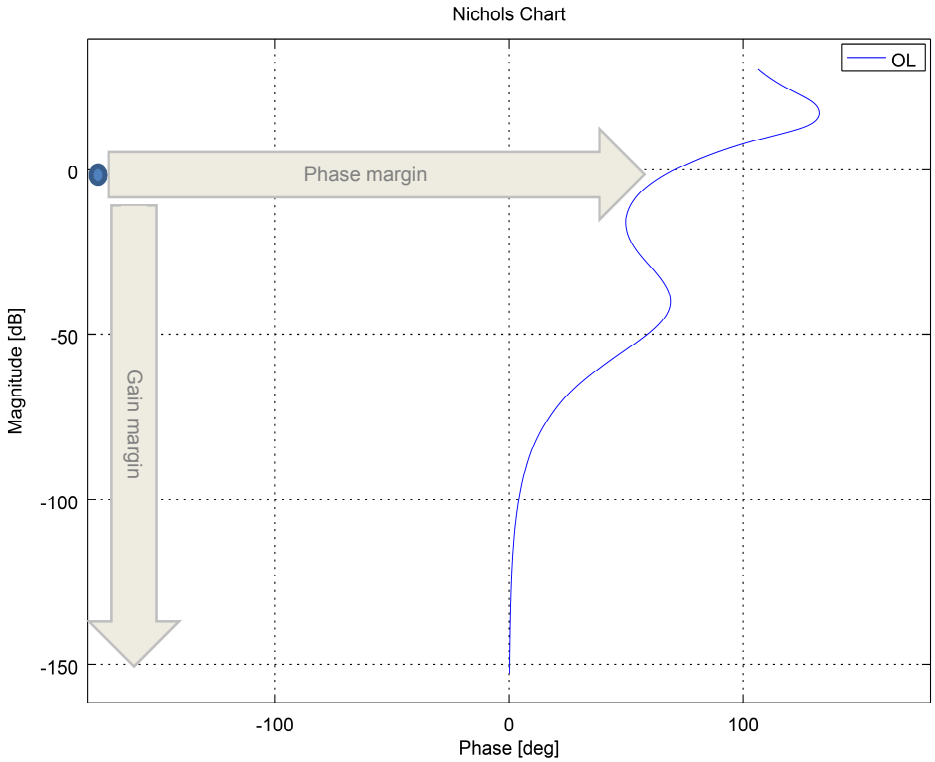

Fig 6. Nichols chart for open loop transfer function GH, case of U3Si2 + SiC

Cladding and Fuel		**Zr cladding**	**SiC cladding**	**Steel cladding**
UO2	Tmax	**219.03**	218.52	219.11
	Most positive pole	**-0.01294**	-0.01294	-0.01294
	Angle of any conjugated poles	**-136.45**	-136.24	-136.34
	Tmax / Tprompt	**1.1893**	1.1866	1.1898
	Gain margin	**inf dB**	inf dB	inf dB
	Phase margin	**252.67**	252.66	252.66
U3Si2	Tmax	226.35	225.77	225.98
	Most positive pole	-0.12920	-0.01292	-0.12920
	Angle of any conjugated poles	-127.00	-127.02	-127.24
	Tmax / Tprompt	1.2291	1.2259	1.2270
	Gain margin	-58.74	-6.97	-49.42
	Phase margin	250.83	250.87	251.16
UN	Tmax	222.76	222.28	223.15
	Most positive pole	-0.01293	-0.01293	-0.01293
	Angle of any conjugated poles	-132.07	-131.98	-132.51
	Tmax / Tprompt	1.2096	1.2070	1.2117
	Gain margin	inf dB	inf dB	inf dB
	Phase margin	251.89	251.88	251.99
UC	Tmax	223.25	222.77	223.35
	Most positive pole	-0.01293	-0.01293	-0.01293
	Angle of any conjugated poles	-131.26	-131.17	-131.18
	Tmax / Tprompt	1.2122	1.2097	1.2128
	Gain margin	inf dB	-11.31	inf dB
	Phase margin	251.73	251.71	251.71

Tab 3: Summary of results

5. Conclusion

Depending on the cladding/pellet combination, results of the dynamic analysis show that pressurized water reactors with ATF may perform somewhat different from typical UO2/Zirconium fuels.

PWR with advanced accident tolerant fuel assemblies considering the fuel and cladding materials in this paper, react to a reactivity perturbation with a power response that does not exhibit repeated oscillations and converges rapidly to a final state where the different sources of reactivity become compensated. The response to any sinusoidal input signal in terms of gain and phase presents the typical PWR characteristics with no important resonances, while they keep the natural frequency of the reactor in a safe range noticeably lower than those frequencies derived from a mechanical source. The main difference arises from the use of the fuel pellet material rather than the cladding material. However, the variations of the dynamic behaviour are small and inherent stability of PWR to reactivity perturbations in a wide range of operating range is preserved.

This work confirms again the self-regulating capability of PWR due to the dynamic combination of fuel and coolant reactivity effects also with nonstandard fuel lattices.

This analysis is based on classical linear stability methods, and it can be complemented with more sophisticated non-linear methods and/or the use of coupled N-TH realistic codes.

6. Nomenclature

P	=	Reactor power, W	UA	=	Heat transfer coefficient, W/m2 K
ρ	=	Reactivity, Δk/k	Wc	=	Core mass flow rate, Kg/s
ρ_{ext}	=	External reactivity, Δk/k	α_f, α_c	=	Fuel and moderator temperature coefficients, Δk/k·K
β	=	Delayed neutron fraction	G	=	Direct reactivity-to-power transfer function
Λ	=	Mean generation lifetime of neutrons, s	H	=	Power-to-feedback reactivity transfer function
λ	=	Delayed neutron decay constant, s	T	=	Total reactivity-to-power transfer function
			Tf	=	Fuel Temperature, K
			Kf	=	Fuel conductivity, W/m.K
C	=	Precursor density	K_{PTF}	=	Fuel temperature gain, K/W
mf, mc	=	Fuel and coolant mass, kg	K_{PTC}	=	Moderator temperature gain, K/W
cpf, cpc	=	Fuel and coolant specific heat, J/kg K	τf	=	Fuel time delay, s
Tf, Tc	=	Fuel and coolant temperature, K	τc	=	Coolant time delay, s
Ti	=	Core inlet temperature, K	τm		Moderator time delay, s
BOC, EOC	=	Beginning, end of cycle			

7. Acknowledgments

Authors wishes to thank ENUSA for the support and availability of tools and time needed for this research work.

8. References

[1] Barret K., Bragg-Sitton,S., Galicki D., “Advanced LWR Nuclear Fuel Cladding System Development Trade-off Study”, page 11, September 2012

[2] Jones R., Lewinsohn C., Senor D., Youngblood G. E., Pacific Northwest National Laboratory, L. L. Snead, Oak Ridge National Laboratory, “Ceramic Matrix Composites”, page 6

[3] IAEA, “Thermophysical Properties of Materials for Nuclear Engineering: A Tutorial and Collection of Data”, page 166, November 2008.

[4] IAEA-TECDOC-1496 , “Thermophysical properties database of materials for light water reactors and heavy water reactors”, pages 29, 91, 105, 115, June 2006

[5] IAEA-TECDOC-643, “Research reactor core conversion guidebook. Volume 4: Fuels (Appendices I-K)”, pages 15, 17, 18,

[6] IAEA, “Thermophysical Properties of Materials for Nuclear Engineering: A Tutorial and Collection of Data”, page 43, November 2008.

[7] Hetrick, D.L., *Dynamics of Nuclear Reactors*, The University of Chicago Press, Chicago (1971).

[8] Weaver, L.E., *Reactor Dynamics and Control - State Space Techniques*, American Elsevier Publishing company, INC., New York (1968).